

Conserved Intergenic Elements and DNA Methylation Cooperate to Regulate Transcription at the *il17* Locus^{*S}

Received for publication, February 10, 2012, and in revised form, May 16, 2012. Published, JBC Papers in Press, June 4, 2012, DOI 10.1074/jbc.M112.351916

Rajan M. Thomas, Hong Sai, and Andrew D. Wells¹

From the Department of Pathology and Laboratory Medicine, Perelman School of Medicine, the University of Pennsylvania and The Children's Hospital of Philadelphia, Philadelphia, Pennsylvania 19104

Background: IL-17 is an inflammatory cytokine that mediates immunopathology in autoimmune disease.

Results: DNA methylation at the *il17* locus is lineage-restricted and blocks STAT3 binding.

Conclusion: Expression of the *il17* genes is regulated by promoter methylation and a novel intergenic enhancer.

Significance: Understanding the mechanisms regulating IL-17 production will facilitate therapeutic control of inflammatory immune responses.

Naive CD4⁺ T cells can differentiate into distinct lineages with unique immune functions. The cytokines TGFβ and IL-6 promote the development of Th17 cells that produce IL-17, an inflammatory cytokine not expressed by other T helper lineages. To further understand how IL-17 production is controlled, we studied an ~120-kb genomic region containing the murine *il17a* and *il17f* genes and seven evolutionarily conserved, intergenic noncoding sequences. We show that the +28-kb noncoding sequence cooperates with STAT3, RORγt, and Runx1 to enhance transcription from both *il17a* and *il17f* promoters. This enhancer and both promoters exhibited Th17 lineage-specific DNA demethylation, accompanied by demethylation of lysine 27 of histone H3 (H3K27) and increased H3K4 methylation. Loss of DNA methylation tended to occur at STAT3 consensus elements, and we show that methylation of one of these elements in the *il17a* promoter directly inhibits STAT3 binding and transcriptional activity. These results demonstrate that TGFβ and IL-6 synergize to epigenetically poise the *il17* loci for expression in Th17 cells, and suggest a general mechanism by which active STAT3 may be epigenetically excluded from STAT3-responsive genes in non-Th17 lineages.

Naive CD4⁺ T cells activated in the presence of TGFβ and IL-6, a physiologic stimulus provided by antigen-presenting cells that phagocytose apoptotic debris from pathogen-infected cells (1), gain the capacity to secrete inflammatory cytokines IL-17A and IL-17F. IL-17F is involved in host defense at mucosal surfaces, whereas IL17A mediates immunity to fungi and bacteria and is involved in autoimmune disease processes such as multiple sclerosis and inflammatory bowel disease (reviewed in Ref. 2). IL-17-producing Th17² cells behave as a distinct

lineage from cells of the Th1, Th2, and regulatory T cell lineages, which do not produce IL-17, suggesting that distinct transcriptional mechanisms may control *il17* gene expression. Genetic studies have established that a combination of STAT3, Runx1, Batf, and IRF4 and the nuclear receptors RORγt, RORα, and Ahr is involved in the induction of IL-17 during Th17 differentiation (reviewed in Ref. 3), but why so many factors are required and how they interact with the genomic architecture of the closely linked *il17a* and *il17f* genes is not known.

We show that the *il17a* promoter is primarily responsive to STAT3 or Runx1, whereas the *il17f* promoter is largely RORγt-responsive, and neither promoter is capable of supporting significant transcriptional cooperativity among these three factors. Cytokine genes are commonly regulated by long distance *cis* regulatory elements (4); therefore, we interrogated seven noncoding sequences (CNS) across an ~120-kb region of the mouse genome encompassing the *il17a* and *il17f* loci and identified two intergenic regions capable of enhancing transcription from the *il17a* and *il17f* promoters. One of these elements is located 5 kb upstream of the *il17a* gene and corresponds to a previously identified enhancer (5). We now show that this enhancer is particularly responsive to RORγt and does not synergize with STAT3 or Runx1. The second element is located between the two *il17* genes, 28 kb downstream of *il17a* and 24 kb downstream of *il17f*. This is a previously unidentified enhancer, and we show that it synergizes with STAT3, RORγt, and Runx1 to drive transcription from both *il17a* and *il17f* promoters.

Like Th17 differentiation from naive CD4⁺ precursors, astrocyte differentiation from neuroepithelial precursors in the developing brain is driven by the combination of a TGFβ family member bone morphogenic protein 2 (BMP2) and an IL-6 family member leukemia inhibitory factor (LIF) (6). LIF/BMP2 cooperativity in this system results in demethylation of STAT3 *cis* elements in astrocyte-specific gene promoters, an epigenetic process required for the astrocyte cell fate decision. We therefore hypothesized that lineage-specific induction of the *il17*

kinase-like orphan receptor; BMP2, bone morphogenic protein 2; LIF, leukemia inhibitory factor; PMA, phorbol 12-myristate 13-acetate; NFAT, nuclear factor of activated T-cells; Ab, antibodies; TSS, transcription start site.

* This work was supported, in whole or in part, by National Institutes of Health Grants AI054643 and AI070807 (to A. D. W.).

^S This article contains supplemental Table 1.

¹ A member of the Fred and Suzanne Biesecker Pediatric Liver Center. To whom correspondence should be addressed: Abramson Research Center, 3615 Civic Center Blvd., Philadelphia, PA 19104. Tel.: 215-590-8710; E-mail: adwells@mail.med.upenn.edu.

² The abbreviations used are: Th, T helper; CNS, conserved noncoding sequence(s); H3K27me3, trimethylation of lysine 27 of histone H3; H3K4me3, trimethylation of lysine 4 of histone H3; ROR, receptor tyrosine

Regulatory Architecture of the *il17* Locus

gene by TGF β and IL-6 in Th17 cells may be regulated by an analogous mechanism. We demonstrate that CpG dinucleotides in the *il17a* promoter, the +28-kb enhancer, and the *il17f* promoter are preferentially demethylated during Th17 lineage commitment and that DNA methylation directly blocks STAT3 binding to a CpG dinucleotide sequence required for full *il17a* promoter activity. These studies demonstrate that the *il17a* and *il17f* genes are regulated transcriptionally by at least two intergenic enhancers, and epigenetically by DNA methylation, which acts as a biochemical switch for STAT3 binding.

EXPERIMENTAL PROCEDURES

Mice—C57BL/6 mice, 4–6 weeks old, were obtained from The Jackson Laboratory and maintained at the laboratory animal facility of The Children's Hospital of Philadelphia. All animal experiments were conducted according to approved institutional protocols and guidelines.

Monoclonal Antibodies—Monoclonal antibodies against CD3 ϵ (2C11) and CD28 (37.51) Ab were purchased from Bio-Express. Mouse recombinant IL-4 and monoclonal Ab against IL-4 (11B11), IFN γ (XMG1), and IL-12 (17.8) were purchased from BD Biosciences. Recombinant IL-12, IL-6, and IL-23 were purchased from eBioscience, TGF β was purchased from R&D Systems, and IL-2 was purchased from Roche Applied Science. Fluorochrome-conjugated mAb used for flow cytometry were purchased from BD Biosciences. All molecular biology reagents were analytical grade and purchased from Sigma-Aldrich.

Vectors—Vectors pGL4-*il17a* containing the 0.6-kb promoter (5), pRc/CMV-STAT3C (7), pTATA-TK-Luc containing four STAT3 binding elements, and retroviral MIGR-ROR γ t were obtained from Addgene. MIGR1-Runx1 was obtained from S. Sakaguchi (Kyoto University, Japan). Control *Renilla*-luciferase vector was obtained from Promega. Mutations were introduced in the STAT3 binding site in the *il17a* 0.6-kb promoter vector using a mutagenesis kit (Stratagene). Conserved noncoding sequence elements surrounding the *il17a*–*il17f* loci were cloned into the *il17a* promoter vector at the XhoI site located at the 5' end of the promoter (supplemental Table 1). The pGL4-*il17f* 0.6-kb promoter construct was generated by cloning the region 0.6 kb upstream of the *il17f* coding region into the XhoI and HindIII sites. CNS elements were subcloned into the XhoI site of the pGL4-*il17f* promoter construct.

Cell Culture—Single cell suspensions of spleen and lymph node were prepared, CD8 $^+$ cells were depleted using Miltenyi CD8 microbeads and columns, and the remaining CD4 $^+$ T cells and antigen presenting cell were cultured with soluble anti-CD3 and anti-CD28 (1 μ g/ml each) for 4 days in the presence of IL-12 (10 ng/ml) and anti-IL-4 Ab (10 μ g/ml) for Th1, with IL-4 (40 ng/ml), anti-IFN γ (10 μ g/ml), and anti-IL-12 (10 μ g/ml) for Th2, with TGF β (5 ng/ml) and IL-2 (20 units/ml) for iTreg, or with anti-IL-4 (20 μ g/ml), anti-IFN γ (20 μ g/ml), TGF β (1 ng/ml), and IL-6 (10 ng/ml) for Th17. In a separate batch of Th17 cultures, IL-23 (10 ng/ml) was also added. After 4 days, cells were harvested, washed, and restimulated for 48 h with plate-bound anti-CD3 and anti-CD28 (1 μ g/ml each). For intracellular staining, restimulated cells were boosted with PMA (10 ng/ml) and ionomycin (1 μ M) for 5 h in the presence of Golgi stop reagent (BD Biosciences). For histone and DNA

methylation analysis, CD4 $^+$ cells were purified from the restimulated cultures (96% purity) using Miltenyi columns.

DNA Methylation—DNA methylation at the *il17a*–*il17f* multilocus region was assessed by sodium bisulfite conversion and cloning as described previously (8). Genomic DNA isolated from T helper cells was treated with sodium bisulfite to convert cytosines to uracil. The *cis* regulatory elements described were PCR-amplified (supplemental Table 1) and cloned into PGEM-T easy vector (Promega), and plasmid DNA isolated from 25–30 clones was sequenced.

Chromatin Immunoprecipitation (ChIP) Analysis—T helper cultures were formaldehyde-fixed, and chromatin was sheared and solubilized by sonication. Chromatin containing histone 3 lysine 4 trimethylation (H3K4me3) and histone 3 lysine 27 trimethylation (H3K27me3) was enriched using specific antibodies (Millipore, Cell Signaling Technologies) and a ChIP assay kit (Millipore), and enriched DNA was purified. *cis* regulatory elements at the *il17* and *ifng* loci were detected in pre-ChIP *versus* post-ChIP fractions and quantified by quantitative PCR (supplemental Table 1) as described (9).

Electrophoretic Mobility Shift Assay (EMSA)—EMSA of STAT3 binding to [γ - 32 P]ATP-labeled double-stranded oligonucleotides representing sequences in the *il17a* promoter containing a STAT3 consensus element was determined using nuclear extracts prepared from Th17 cells. To check the methylation effect on STAT3 binding, a methylated probe was synthesized by incorporating the cytosine methylation at a CpG site located within the STAT3 binding element. EMSA reactions were performed as described previously (10).

Oligonucleotide Pulldown Assay—Oligonucleotide probes used for EMSA analysis were 5' end-labeled with biotin and incubated (0.5 μ M) with total cell lysate (400 μ g) prepared from stimulated Th17 cells under the same ionic conditions used in EMSA reactions. Magnetic streptavidin-conjugated agarose beads (MagSelect, Sigma-Aldrich) were used to collect protein complexes bound to the DNA probes. Beads were washed following the protocol provided by the vendor, bound protein complexes were eluted with Laemmli buffer, and STAT3 was visualized by immunoblot using antibody (C-20) purchased from Santa Cruz Biotechnologies.

Transient Promoter-Reporter Assays—293T or EL4 cells were transfected with wild-type or mutant 0.6-kb *il17a* promoter-luciferase vectors for 48 h and stimulated with PMA (30 ng/ml) and ionomycin (1 μ M) for 5 h before harvesting. *Renilla* luciferase driven by a constitutive vector was used to normalize the transfection. Transfection experiments were performed with cells co-transfected with STAT3C (constitutively active form), Runx1, or ROR γ t. STAT3-negative and STAT3-positive reporter luciferase vectors were used as positive and negative controls for STAT3 transfections. Bioluminescence produced by firefly *versus Renilla* luciferase was estimated using cell lysate prepared from the transfected cells by a Dual-Luciferase assay kit purchased from Promega.

RESULTS

Lineage-specific Histone Methylation across the *il17a* and *il17f* Loci in Th17 Cells—To study the epigenetic processes associated with induction *versus* silencing of *il17* gene expres-

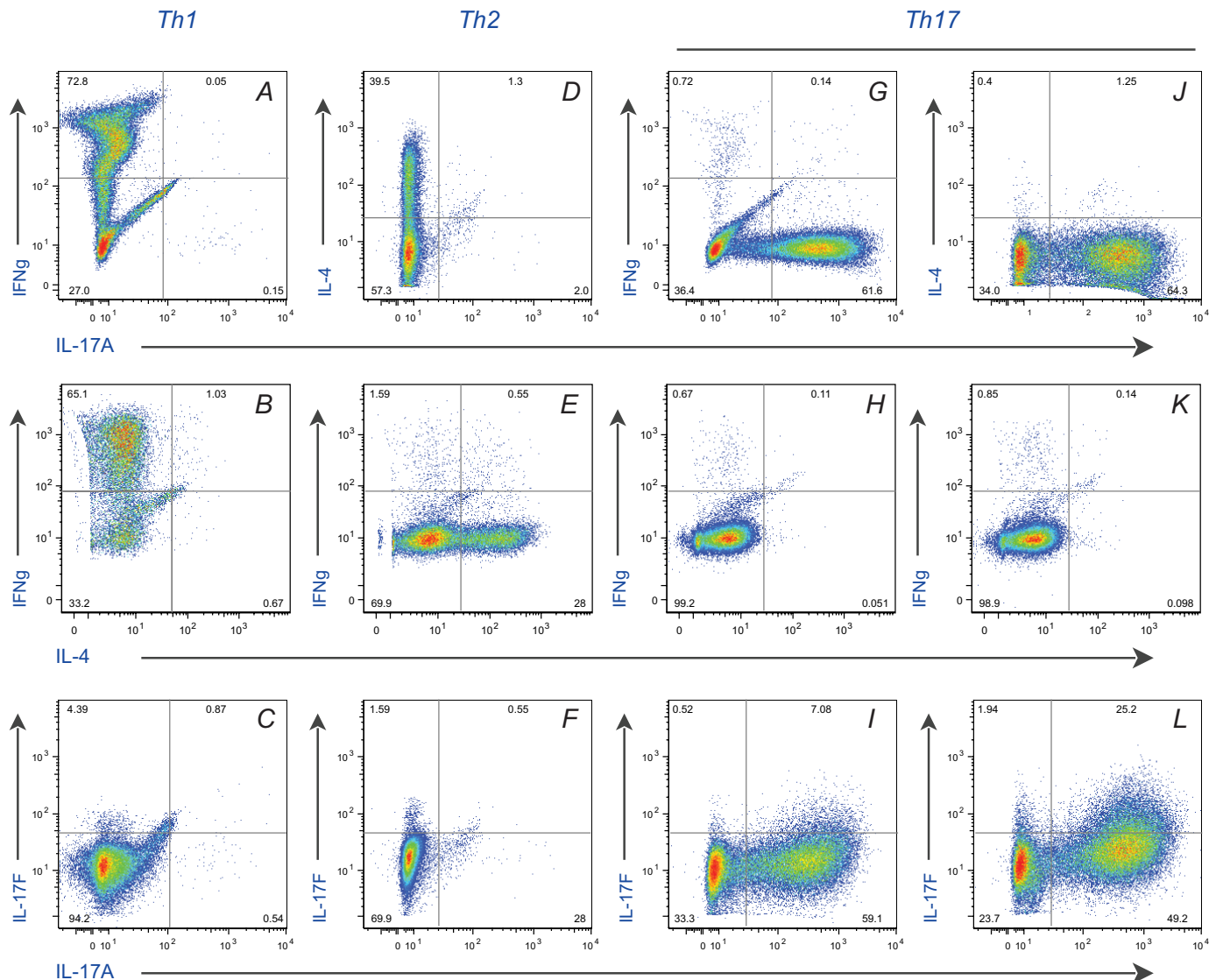


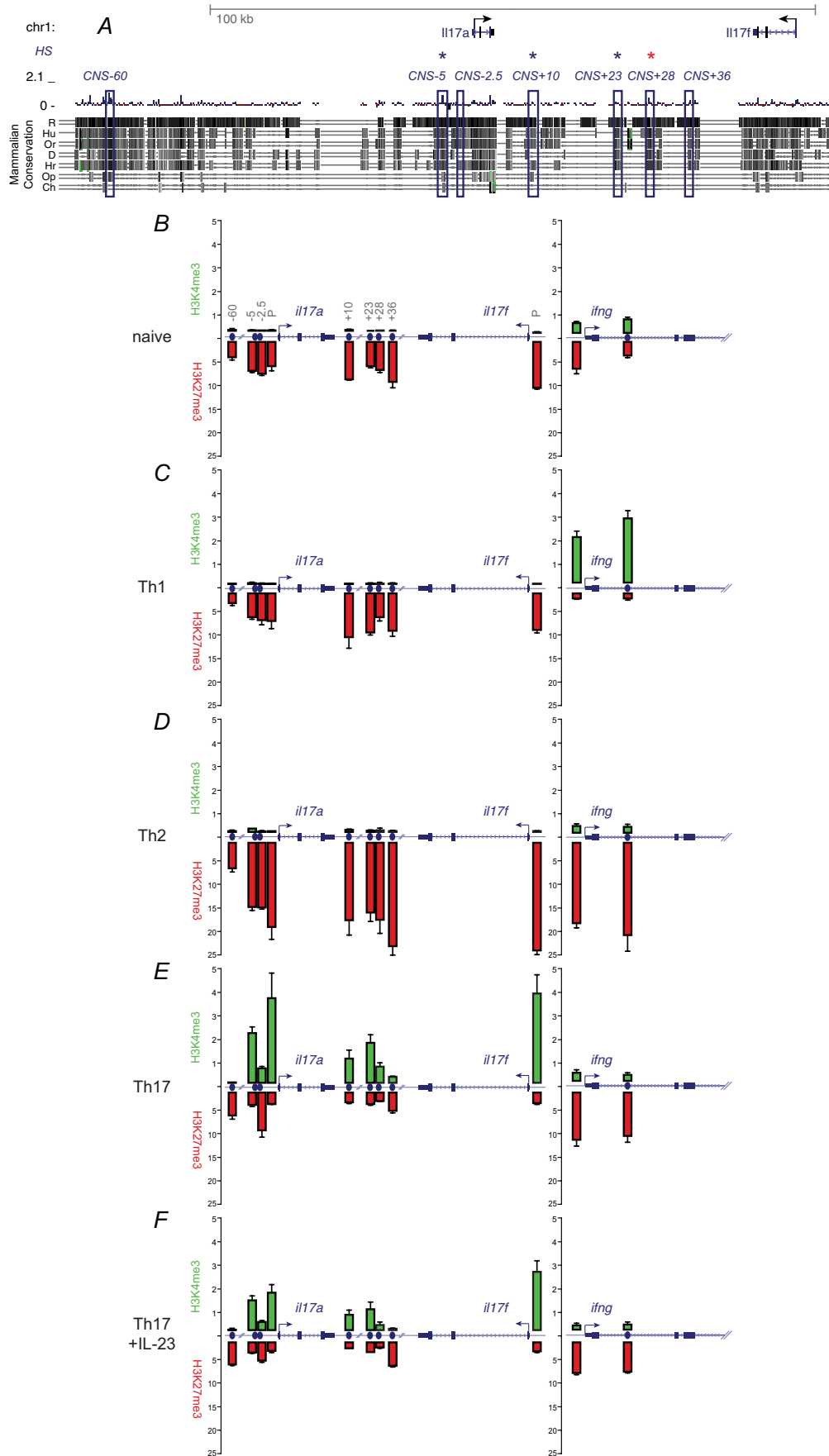
FIGURE 1. **Mutually exclusive patterns of cytokine production in Th1, Th2, and Th17 cells.** CD8-depleted spleen and lymph node cells were stimulated *in vitro* with soluble anti-CD3/28 Ab in the presence of IL-12 and anti-IL-4 (Th1, A–C), IL-4 and anti-IL-12 (Th2, D–F), or TGF β , IL-6, anti-IFN γ and anti-IL4 (Th17, G–I) for 4 days. In a separate Th17 culture, IL-23 was also added (J–L). Cells were then restimulated with plate-bound anti-CD3/28 under neutral conditions, and IFN γ , IL-4, IL-17A, and IL-17F production was assessed by intracellular staining and flow cytometry. Data are representative of four independent experiments.

sion in differentiating CD4⁺ helper T cells, we generated Th1, Th2, and Th17 cells *in vitro*. As expected, when restimulated under neutral conditions, Th1 cells produced IFN γ but not IL-4, IL-17A, or IL-17F (Fig. 1, A–C), Th2 cells produced IL-4 but not IFN γ , IL-17A, or IL-17F (Fig. 1, D–F), and Th17 cells produced IL-17A and IL-17F but not IFN γ or IL-4 (Fig. 1, G–I). The cytokine IL-23 has been reported to enhance Th17 differentiation and is required for pathogenicity *in vivo* (11, 12). The addition of IL-23 to Th17 cultures did not influence IL-17A production, but augmented the secretion of IL-17F (Fig. 1, J–L).

To identify potential *cis* regulatory elements for the *il17a* and *il17f* loci, we measured methylation of lysine 4 of histone H3 (H3K4me3), a chromatin mark associated with gene activity or expression potential, and methylation of lysine 27 of histone H3 (H3K27me3), a chromatin mark associated with active gene silencing (reviewed in Ref. 13), at several defined (14, 15) evolutionarily conserved CNS surrounding the *il17a* and *il17f* genes (Fig. 2A). Naive CD4⁺ T cells exhibited significant

H3K27 trimethylation at the *il17a* and *il17f* promoter regions and at CNS regions –60, –5, –2.5, +10, +23, +28, and +36 kb from the *il17a* TSS (Fig. 2B, left panel). The levels of H3K27me3 at the *il17* loci were as high or higher than that observed at the *ifn γ* locus in naive cells (Fig. 2B, right panel). Although a small amount of H3K4 trimethylation could be detected near the *ifn γ* gene, the *il17* multilocus regions was completely devoid of this mark. The chromatin at the *il17a* and *il17f* loci was maintained in this same configuration in differentiated Th1 cells (Fig. 2C), whereas the *ifn γ* locus exhibited the expected increase in H3K4me3 and a loss of H3K27me3. Th2 cells strongly silenced both of these genomic regions (Fig. 2D). Similar to previous studies (14, 16), we observed strong trimethylation of H3K4 at the *il17a* and *il17f* promoters, as well as at the –5, +10, +23, and +28 CNS, but not at the –60 CNS (Fig. 2E). The increase in H3K4 methylation was accompanied by a significant loss of the opposing H3K27me3 mark, except at –60 and –2.5 CNS, which maintained naive levels of the silencing H3K27me3

Regulatory Architecture of the *il17* Locus



mark. Conversely, the *ifn γ* locus in these cells did not accumulate H3K4me₃, but instead was subjected to increased methylation at lysine 27. Th17 cells cultured with IL-23, which led to increased IL-17F secretion (Fig. 1L), retained strong H3K4me₃ levels at the *il17f* promoter, but actually reduced H3K4 trimethylation at the *il17a* locus (Fig. 2F). These results highlight intergenic regions that may be involved in the transcriptional control of the *il17a* and *il17f* loci and indicate that these genes are subject to epigenetic regulation at the level of chromatin remodeling.

The +28 Intergenic CNS Is a STAT3-, ROR γ t-, and Runx1-responsive Enhancer for *il17* Transcription—To determine whether the CNS regions analyzed in Fig. 2 are directly involved in the regulation of *il17* gene transcription, we cloned each CNS (Fig. 3A) in front of the *il17a* promoter or the *il17f* promoter and tested the capacity of these DNA elements to drive luciferase activity upon transient transfection in 293T cells. As reported previously (5, 17), the 0.6-kb *il17a* promoter was moderately active by itself in unmanipulated cells (Fig. 3D, yellow bars), and none of the CNS regions were able to augment transcription under these conditions (Fig. 3D, green to blue bars). IL-6 induces *il17a* gene expression through the activation of STAT3 (18, 19); therefore, we tested whether the CNS regions surrounding the *il17a* and *il17f* genes were responsive to the activity of this transcription factor. Co-transfection with a constitutively active form of STAT3 (STAT3C (Ref. 7)) resulted in increased promoter activity (Fig. 3D, yellow bars), and the +28 CNS was the only one of the seven conserved regions able to further enhance *il17a* promoter-driven transcription under these circumstances (Fig. 3D, blue bars). Consistent with this, *in silico* analysis of the +28 CNS sequence identified a strong STAT3 consensus element (Fig. 3C), and a previous genome-wide ChIP analysis indicates that STAT3 is bound to this region in Th17 cells (20). The transcription factor ROR γ t is specifically induced during Th17 differentiation and is required for *il17* gene expression (21); therefore, we tested whether the CNS regions surrounding the *il17a* and *il17f* genes were responsive to the activity of this transcription factor. The -5 CNS was recently shown to contain an ROR consensus element (Fig. 3F) and to enhance *il17a* promoter activity in response to ROR γ t (5). Consistent with this study, we found that co-transfection with ROR γ t did not affect minimal promoter activity (Fig. 3D, yellow bars), but the promoter became ROR γ t-responsive when linked to -5 CNS (Fig. 3D, green bars). However, in addition to the -5 CNS, we find that the +28 CNS is also able to cooperate with ROR γ t to drive transcription from the *il17a* promoter (Fig. 3D, blue bars). Consistent with the fact that the +28 CNS, but not the -5 CNS, contains consensus elements for both STAT3 and ROR (Fig. 3, B and C), the +28 CNS was the only region capable of enhancing transcription over that of the minimal promoter when co-transfected with both STAT3C and ROR γ t (Fig. 3E, blue bars). The +28 enhancer also contains

multiple putative binding sites for Runx1/AML1 (Fig. 3C), another factor known to transactivate the *il17a* promoter (5); therefore, we tested whether this enhancer is responsive to Runx1. The promoter itself was moderately responsive to Runx1 when expressed alone (Fig. 3E, yellow bars in empty vector versus Runx1), but neither the -5 CNS nor the +28 CNS was able to significantly enhance transcription under these conditions (Fig. 3E, green and blue bars). Likewise, when Runx1 was co-expressed with ROR γ t, it did not drive transcription from any of the promoter-enhancer constructs significantly more than ROR γ t did by itself (Fig. 3E, ROR γ t versus Runx1+ROR γ t). However, Runx1 was able to cooperate strongly with STAT3 at both the promoter (Fig. 3E, yellow bars in Runx1 + STAT3) and the +28 enhancer (Fig. 3E, blue bars in Runx1 + STAT3) to drive *il17a* promoter activity to levels 4–5-fold higher than in the presence of either Runx1 or STAT3 alone.

Like the *il17a* promoter, the *il17f* promoter was also moderately responsive to STAT3 (Fig. 3F, yellow bars). However, unlike *il17a*, none of the intergenic CNS elements, including the +28 element, was able to further enhance *il17f* promoter activity under these conditions (Fig. 3F, STAT3C). The *il17f* promoter was likewise unresponsive to Runx1 (Fig. 3G, yellow bars in Runx1), and neither the -5 nor the +28 CNS elements were able to enhance *il17f* transcription in the presence of this transcription factor (Fig. 3G, green and blue bars in Runx1). The *il17f* promoter was responsive to ROR γ t (Fig. 3, F and G, yellow bars in ROR γ t), and both the -5 and the +28 CNS were able to further enhance *il17f* promoter activity in the presence of this transcription factor (Fig. 3, F and G, green and blue bars in ROR γ t). Unlike at the *il17a* promoter, ROR γ t was unable to synergize with STAT3 or Runx1 to drive transcription from the *il17f* promoter (Fig. 3G). These data indicate that STAT3, ROR γ t, and Runx1 synergize to transactivate the *il17a*/-5/+28 promoter-enhancer unit, whereas the *il17f*/-5/+28 promoter-enhancer unit is largely responsive to ROR γ t. These data establish the +28 CNS as an intergenic *cis* regulatory element that undergoes lineage-specific chromatin remodeling in Th17 cells and is capable of coordinating the activities of STAT3, ROR γ t, and Runx1 to enhance transcription from the *il17a* and *il17f* promoters.

Lineage-specific Demethylation of DNA at the +28 Enhancer and the *il17a* and *il17f* Promoters in Th17 Cells—Another important mode of epigenetic regulation occurs at the level of DNA methylation at CpG dinucleotides. CpG islands, defined as a >200-bp region with >55% GC content, are often found at *cis* regulatory regions and are used by cells to nucleate DNA methylation machinery at silenced genes (22). The *il17* multilocus region is devoid of CpG islands; however, the *il17a* promoter, the +28 enhancer, and the *il17f* promoter regions each contain approximately a dozen CpG dinucleotides (Fig. 4). Therefore, we measured DNA methylation at these elements to

FIGURE 2. Chromatin modifications at the *il17a*–*il17f* multilocus region in T helper lineages. A, mammalian evolutionary conservation surrounding the murine *il17a* and *il17f* loci. Conserved CNS at -60, -5, -2.5, +10, +23, +28, and +36 kb from the *il17a* TSS are boxed. Lineage-specific DNase hypersensitivity sites (HS) identified by Mukasa *et al.* (14) are indicated by a blue asterisk for activated Th17 cells and by a red asterisk for resting Th17 cells. Trimethylation of lysine 27 of histone H3 (H3K27me₃, red) and trimethylation of lysine 4 of histone H3 (H3K4me₃, green) at each CNS of the *il17a*-f loci (left panels) or the promoter and intronic enhancer of the *ifn γ* locus (right panels) are depicted for naive (B), Th1 (C), Th2 (D), Th17 (E), and Th17 plus IL-23 (F) cells generated *in vitro* as in Fig. 1. Data are representative of two independent experiments. Error bars indicate S.D.

Regulatory Architecture of the *il17* Locus

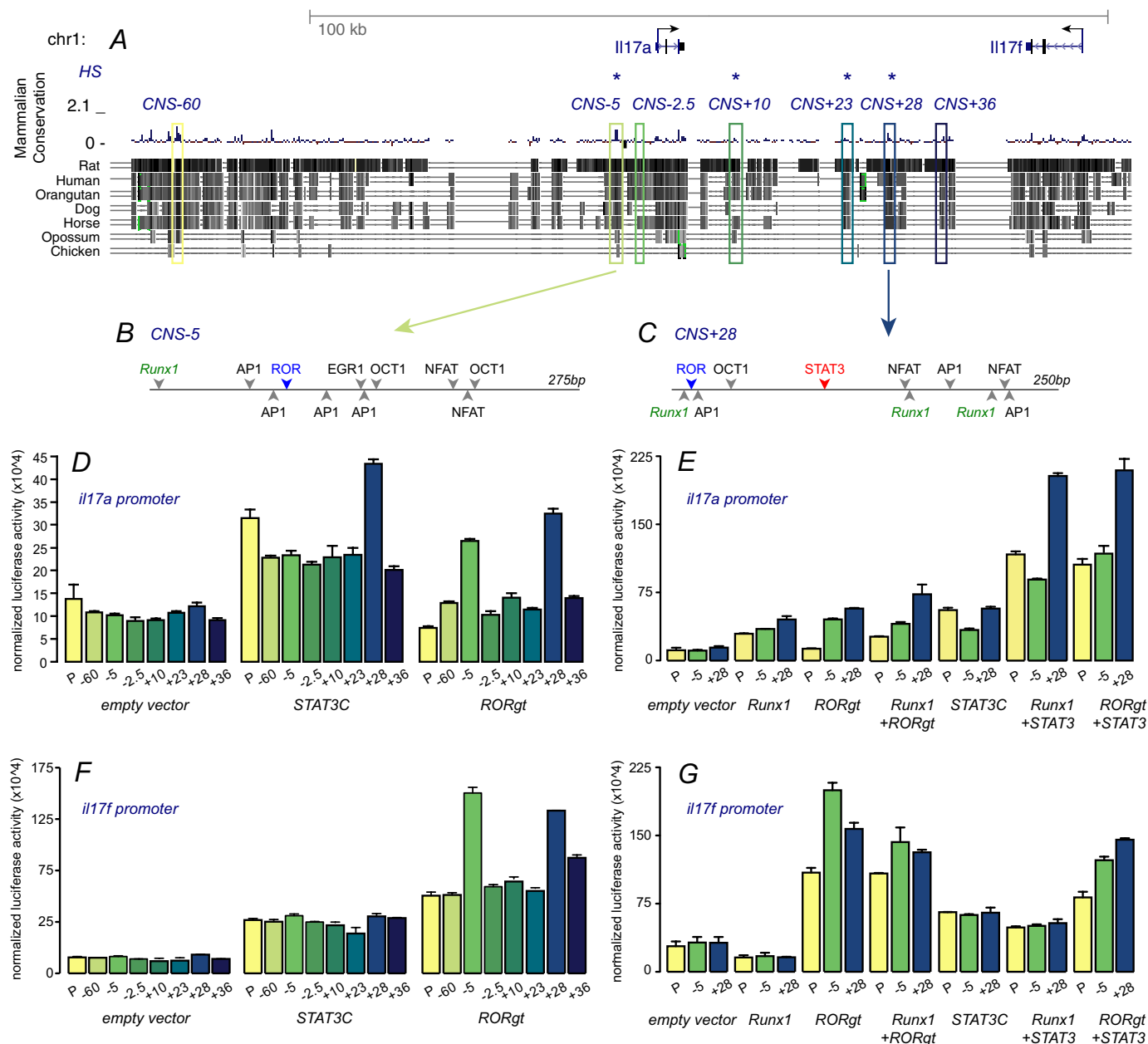


FIGURE 3. Transcriptional enhancement by CNS within the *il17a*–*il17f* multilocus region. *A*, conserved, intergenic sequences surrounding the *il17a* and *il17f* loci (boxed in yellow to blue). *HS*, hypersensitivity sites. *B–C*, *in silico* Transcription Element Search System (TESS) analysis of the –5- (*B*) and +28- (*C*) CNS regions is depicted. Individual CNS were cloned upstream of the –0.6-kb *il17a* promoter (*D* and *E*) or the –0.6-kb *il17f* promoter (*F* and *G*) driving firefly luciferase. Each promoter-luciferase construct (yellow bars), or CNS-promoter-luciferase construct (green to blue colored bars) was co-transfected together with a *Renilla* control and empty vector, constitutively active STAT3 (STAT3C), or ROR γ t into 293T cells (*D* and *F*), and luciferase activity was measured 48 h after stimulation with PMA/ionomycin. Firefly luciferase activity was normalized against constitutive *Renilla* luciferase activity for each sample. In a separate experiment, Runx1, STAT3C, or ROR γ t was co-transfected, either individually or in combination, with –5 CNS or +28 CNS linked to the *il17a* (*E*) or *il17f* (*G*) promoters, and luciferase activity was measured as in *D* and *F*. Data are representative of four independent experiments. Error bars indicate S.D.

determine whether this epigenetic mark is regulated in a lineage-specific manner in T helper cells.

CpG dinucleotides within the ~650-bp region upstream of the *il17a* TSS (Fig. 4A), an ~300-bp region including the +28 enhancer (Fig. 4B), and the region ~200–500 bp upstream of the *il17f* TSS (Fig. 4C) were all highly methylated (at frequencies of 80–100%) in naive CD4⁺ T cells (Fig. 4, first row). During Th1 and Th2 differentiation, CpG at the *il17a* and *il17f* promoters remained highly methylated, with the exception of the –33 dinucleotide adjacent to the TATA box (Fig. 4A, second and third rows) and the –245 dinucleotide in the *il17f* promoter

(Fig. 4C, second and third rows), which were 60–70% methylated in these lineages. Th1 cells exhibited significant loss of methylation at the +28 enhancer (Fig. 4B, second row), whereas methylation was largely maintained in Th2 cells (Fig. 4B, third row). Conversely, differentiating Th17 cells exhibited a 80–90% loss of DNA methylation across an ~175-bp region of the *il17a* promoter (Fig. 4A, fourth row) and across an ~250-bp region upstream of the *il17f* gene (Fig. 4C, fourth row). The +28 enhancer also exhibited a marked loss of DNA methylation at CpG dinucleotides in Th17 cells, to a much larger extent than that observed in Th1 or Th2 cells (Fig. 4B, fourth row). The

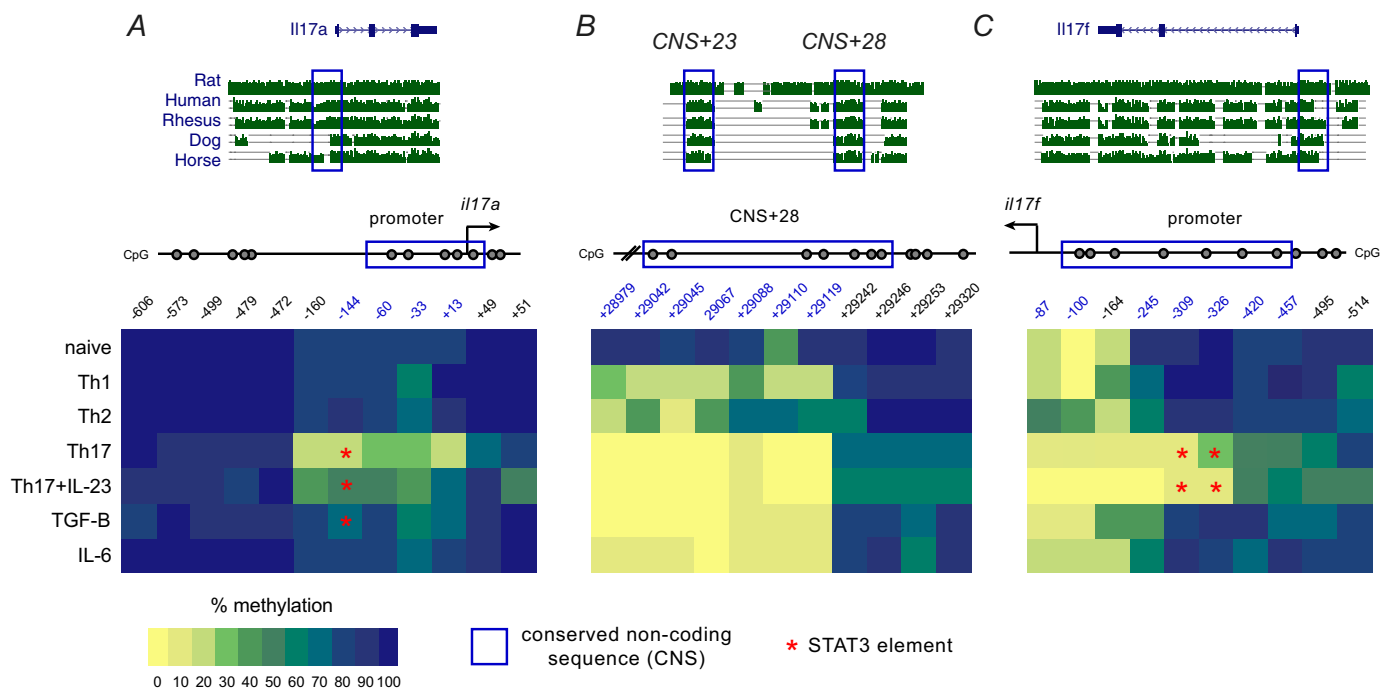


FIGURE 4. DNA methylation at the *il17a* and *il17f* loci in T helper lineages. Evolutionarily conserved CpG dinucleotides (gray circles) within the *il17a* promoter (A), +28 CNS region (B), and *il17f* promoter (C) are boxed in blue. Bisulfite conversion sequence analysis of DNA methylation in naive (row 1), Th1 (row 2), Th2 (row 3), Th17 (row 4), Th17 plus IL-23 (row 5), and iTreg (row 6) cells and cells stimulated with IL-6, anti-IFN γ , and anti-IL-4 (row 7) is depicted by a heat map where blue represents 100% methylation at a given CpG, and yellow represents 0% methylation. Red asterisks indicate STAT3 consensus elements.

addition of IL-23, which selectively enhanced the secretion of IL-17F by Th17 cells (Fig. 1), caused preferential demethylation of the *il17f* promoter, particularly at the -326 CpG (Fig. 4C, fifth row). These data suggest that DNA demethylation at the *il17* loci facilitates *il17* gene expression.

In this *in vitro* culture model, Th17 differentiation is driven by the combination of TGF β and IL-6 (in the presence of neutralizing Ab to IFN γ and IL-4). To determine the contribution of TGF β receptor-coupled signaling versus IL-6 receptor-coupled signaling to the demethylation of DNA observed at the *il17* loci in the Th17 lineage, we stimulated naive CD4⁺ T cells under the same Th17 culture conditions described above, except that either IL-6 was omitted (Fig. 4, sixth row) or TGF β was omitted (Fig. 4, seventh row). Neither signals from IL-6 in the absence of TGF β nor signals from TGF β in the absence of IL-6 were able to induce full DNA demethylation at the *il17a* or *il17f* promoters (Fig. 4, A and C). However, TGF β , which in the absence of IL-6 promotes regulatory T cell differentiation, was able to mediate partial demethylation of the *il17a* -144 CpG (Fig. 4A, sixth row). Furthermore, demethylation at the +28 CNS occurred in cells cultured in either TGF β alone (Fig. 4B) or cells cultured with IL-6 alone (Fig. 4B). These data suggest that TGF β by itself may be capable of partial epigenetic priming of the *il17* loci, but that full demethylation of the *il17a*-*f* multilocus region and commitment to the Th17 lineage require the action of both cytokines.

STAT3 Binding to the *il17a* Promoter Is Lineage-restricted and Is Inhibited by DNA Methylation—Interestingly, the most drastic drop in DNA methylation in the Th17 lineage tended to occur at CpG dinucleotides within consensus elements for STAT3, e.g. -144 in the *il17a* promoter and -309 and -326 in the *il17f* promoter (Fig. 4, A and C, red asterisks). This led us to

hypothesize that DNA methylation at STAT3 *cis* elements in non-Th17 cells inhibits STAT3 binding at the *il17* genes. The minimal *il17a* promoter contains a putative STAT3 binding site at -144 (CCGTCA), and our results in Fig. 3 show that this promoter is STAT3-responsive. To determine whether this element directly contributes to the transcriptional activity of the *il17a* promoter, we mutated the second cytosine of this element to thymidine (CTGTCA), a substitution (indicated by bold) that would be expected to reduce the affinity of this sequence for STAT3 (23). When transiently transfected into EL-4 cells, the wild-type promoter was moderately active and was responsive to stimulation with PMA, ionomycin, and IL-6 (Fig. 5A, dark gray bars). The C \rightarrow T mutation in the -144 element resulted in a 50–70% reduction in promoter activity under both resting and stimulated conditions (Fig. 5A, light gray bars). To specifically determine the effect of this mutation on STAT3 activity, we utilized constitutively active STAT3C. The wild-type *il17a* promoter showed moderate activity in 293T cells and was increased 2-fold when co-transfected with STAT3C (Fig. 5B, dark gray bars). However, when co-transfected with a promoter containing the mutated -144 element, the stimulatory activity of STAT3 was abrogated (Fig. 5B, light gray bar). These data demonstrate that the STAT3 consensus element at -144 is required for full *il17a* promoter activity; therefore, we tested whether DNA methylation of this element influences STAT3 binding.

To examine STAT3 binding in this region, we first measured STAT3 binding to the endogenous *il17a* promoter in primary T helper subsets by chromatin immunoprecipitation analysis. Consistent with a previous study (24), we detected strong binding of native STAT3 to the *il17a* promoter in activated Th17 cells (Fig. 5C). However, to test whether STAT3 occupancy at

Regulatory Architecture of the *il17* Locus

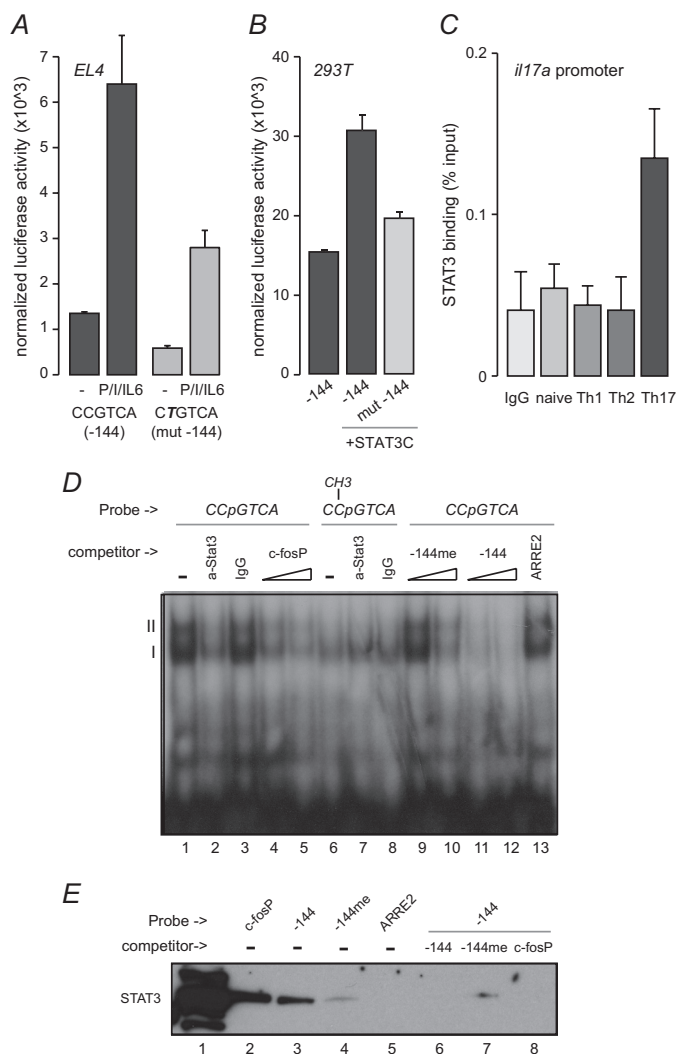


FIGURE 5. Lineage-specific, methylation-sensitive binding of STAT3 contributes to transcriptional activity of the *il17a* promoter. **A**, EL4 cells were transfected with a wild-type ~ 0.6 -kb *il17a* promoter-luciferase construct (dark gray bars) or a mutant *il17a* promoter construct with a C \rightarrow T substitution in the -144 STAT3 element (light gray bars). Cells were cultured with or without PMA, ionomycin, and IL-6, and luciferase activity was normalized to *Renilla* for each sample. **B**, 293T cells were co-transfected with wild-type (dark gray bars) or mutant (mut) (light gray bar) *il17a* promoter-luciferase and either control empty vector (lane 1) or STAT3C (lanes 2 and 3). Luciferase activity was normalized to *Renilla* as in **A**. **C**, primary naive, Th1, Th2, and Th17 CD4⁺ cells were assessed for *in vivo* STAT3 occupancy at the endogenous *il17a* promoter by ChIP analysis. Error bars indicate S.D. **D**, *in vitro* binding activity from 10 μ g of nuclear extracts of primary Th17 cells was assessed by EMSA using radiolabeled probes comprising the unmethylated (CCGTCA, lanes 1–5 and 9–13) or methylated (CC(CH3)GTCA, lanes 6–8) -144 STAT3 element. Two specific DNA-protein complexes (I and II) are indicated. Also added to the binding reactions were anti-STAT3 (lanes 2 and 7) or nonspecific IgG (lanes 3 and 8) antibody or 250 nM (lanes 4, 9, and 11) or 500 nM (lanes 5, 10, and 12) unlabeled *c-fos* STAT3 element (lanes 4 and 5), methylated -144 element (lanes 9 and 10), unmethylated -144 (lanes 11 and 12), or control NFAT/AP-1 binding site from the *il2* promoter ARRE-2 element (lane 13). **E**, *in vitro* binding of STAT3 from extracts of primary Th17 cells (400 μ g) to the positive control *c-fos* promoter STAT3 element (lane 2), unmethylated -144 (lane 3), methylated -144 (lane 4), or control ARRE-2 element (lane 5) was assessed by DNA affinity precipitation followed by SDS-PAGE and anti-STAT3 immunoblot analysis. Relative binding affinities were determined by the addition of a 2-fold molar excess of unbiotinylated unmethylated -144 oligonucleotide (lane 6), methylated -144 oligonucleotide (lane 7), or *c-fos* STAT3 oligonucleotide (lane 8) to biotinylated -144 + cell extract binding reactions. STAT3 in whole nuclear extracts prior to binding is shown in lane 1. Data are representative of two independent experiments.

the *il17a* promoter is lineage-restricted, we also examined STAT3 binding in naive, Th2, and Th1 cells. As expected, no STAT3 occupancy was detected in naive CD4⁺ T cells or activated Th2 cells (Fig. 5C). However, we also failed to detect STAT3 binding at the *il17a* promoter in activated Th1 cells (Fig. 5C) despite the fact that IL-12 activates STAT3 in addition to STAT4 in murine Th1 cells (25). These data suggest that a gene-proximal checkpoint restricts STAT3 binding to the *il17a* promoter in non-Th17 cells.

To directly test whether methylation of the *il17a* promoter opposes STAT3 DNA binding, we probed nuclear extracts of primary Th17 cells with a radiolabeled dsDNA oligonucleotide representing the putative -144 STAT3 element (CCpGTCA) from the *il17a* promoter using an electrophoretic mobility shift approach. This sequence, which simulates the unmethylated -144 site as it would exist in Th17 cells (*i.e.* Fig. 4A), formed two protein-DNA complexes (Fig. 5D, lane 1, I and II). Formation of both complexes was inhibited by the addition of an anti-STAT3 antibody (Fig. 5D, lane 2), but not by an irrelevant control antibody (Fig. 5D, lane 3), and a defined STAT3 element from the *c-fos* promoter could effectively compete with the -144 element for binding to both complexes (Fig. 5D, lanes 4 and 5). These data demonstrate a sequence-specific, STAT3-dependent binding activity toward the -144 *il17a* promoter element in Th17 cells. To simulate the -144 STAT3 site as it would exist in non-Th17 cells (*i.e.* Fig. 4A), we used an oligonucleotide that was synthetically methylated at the CpG dinucleotide (CC(CH3)pGTCA) to probe Th17 nuclear extracts. This methylated STAT3 oligonucleotide completely failed to form complex II and exhibited a reduced capacity to form complex I (Fig. 5D, lanes 6–8). Indeed, although the unmethylated -144 element competed very effectively with its own binding (Fig. 5D, lanes 11 and 12), the methylated form was a much less efficient competitor of the unmethylated element binding activity (Fig. 5D, lane 9), comparable with a control NFAT/AP-1 site in the ARRE-2 element from the *il2* promoter (Fig. 5D, lane 13), and only showed partial inhibition of -144 binding at greater excess (Fig. 5D, lane 10). These EMSA data show that methylation of the -144 STAT3 element in the *il17a* promoter greatly reduces its binding affinity.

In a separate approach, we coupled the unmethylated CCpGTCA or methylated CC(CH3)pGTCA oligonucleotides to streptavidin beads. These beads were then incubated with extracts from Th17 cells, washed, and subjected to SDS-PAGE followed by immunoblot analysis with an antibody specific for STAT3. These experiments showed that native STAT3 from Th17 cells binds to the unmethylated -144 *il17a* promoter element (Fig. 5E, lane 3) with an affinity comparable with the binding of STAT3 to a defined STAT3 element from the *c-fos* promoter (Fig. 5E, lane 2). This binding was sequence-specific as a control NFAT/AP-1 site in the ARRE-2 element from the *il2* promoter was unable to precipitate STAT3 (Fig. 5E, lane 5). However, STAT3 exhibited greatly reduced binding to the methylated -144 *il17a* promoter element (Fig. 5E, lane 4). Furthermore, although the *c-fos* STAT3 element and the unmethylated -144 element efficiently competed with -144 for binding to STAT3 (Fig. 5E, lanes 6 and 8), the methylated -144 was a less efficient competitor of STAT3 binding to the unmethylated

lated -144 element (Fig. 5E, lane 7). These data demonstrate that the -144 CpG, which is demethylated specifically in differentiating Th17 cells, resides in a *bona fide* STAT3 binding element that is required for full *il17a* promoter activity. Binding of STAT3 to this element is inhibited by DNA methylation, establishing this process as an epigenetic switch that regulates *il17* gene expression during T helper differentiation.

DISCUSSION

In this study, we show that the closely linked *il17a* and *il17f* loci exhibit Th17 lineage-specific epigenetic modification of histones and DNA. In particular, marked DNA demethylation occurred at the *il17a* promoter, at the *il17f* promoter, and at an intergenic conserved noncoding sequence +28 kb from the *il17a* gene in CD4⁺ T cells stimulated in the presence of both TGF β and IL-6. One of the CpG dinucleotides preferentially demethylated in Th17 cells is located within a STAT3 consensus element in the *il17a* promoter. We show that this element is a *bona fide* STAT3 binding site, that this element is required for full *il17a* promoter activity, and that DNA methylation at this site abrogates STAT3 binding.

These data suggest that CD4⁺ T cells use methylation of STAT3 DNA elements in cell type-specific promoters as an epigenetic switch for regulation of cell fate decisions during an immune response. An analogous mechanism has been shown to regulate the astrocyte *versus* neuronal cell fate decision during brain development (6). Similar to Th17 differentiation from naive CD4⁺ T cells, astrocyte differentiation from neuroepithelial precursors is driven by the combined action of the IL-6 family member LIF and the TGF β family member BMP2. Combined LIF-BMP2 signaling leads to demethylation of a STAT3 element in the promoter of the gene encoding the glial fibrillary acidic protein (GFAP), a STAT3-dependent factor required for astrocyte differentiation. We therefore hypothesized that TGF β receptor-coupled morphogenic signals during T cell activation might lead to the initial demethylation of STAT3 elements in the *il17a* and *il17f* promoters, whereas IL-6 would induce the STAT3 activity required to transactivate these and other Th17-specific genes. We tested this and found that TGF β in the absence of IL-6 was able to mediate full demethylation of the +28-kb enhancer and partial demethylation of the STAT3 element in the *il17a* promoter (Fig. 4). This partial priming of the *il17* locus provides an explanation for previous results in which CD4⁺ T cells expressing constitutively active STAT3 exhibited IL-17 production when stimulated with TGF β in the absence of IL-6 (18, 19). However, IL-17 production under these circumstances was still ~10-fold lower than that produced by cells stimulated with TGF β and IL-6, suggesting that STAT3-independent IL-6 receptor signaling may be involved and/or that the residual DNA methylation at the *il17a-f* loci under these conditions can oppose STAT3 activity.

The cytokine IL-23 is required for *in vivo* Th17 function, but IL-6 can substitute for its activity *in vitro* (19). Consistent with this, we found that IL-23 did not influence IL-17A production in TGF β plus IL-6 cultures, but did augment IL-17F secretion in a manner associated with reduced DNA methylation at the -326 STAT3 consensus element in the *il17f* promoter. IL-23 has also been shown to promote the appearance of IFN γ -pro-

ducing Th17 cells *in vivo* during the development of experimental autoimmune encephalitis (26). However, we found no effect of IL-23 on either histone or DNA methylation at the *ifn γ* locus in our short term *in vitro* Th17 cultures,³ suggesting that IL-23 acts indirectly to promote IFN γ production by Th17 cells *in vivo* or that factors in addition to IL-23 are required for this phenomenon.

A combination of several transcription factors including STAT3, ROR γ t, and Runx1 is required to induce *il17* expression. Deletional analysis of the *il17a* promoter by Ichiyama *et al.* (17) indicated that the core promoter is contained within the first ~300 bp of the region upstream of the TSS, and Zhang *et al.* (5) found that inclusion of sequences up to -2 kb increased transcriptional activity. Whether the -2-kb region is a *bona fide* part of the promoter *versus* a proximal enhancer (e.g. like the *il2* promoter/enhancer) was not determined; therefore, we chose to use the -0.6-kb region as the promoter in our studies. We find that the -0.6-kb *il17a* promoter contains a *bona fide* STAT3 *cis* element and is highly STAT3-responsive, whereas it is not responsive to ROR γ t and is only mildly responsive to Runx1. The *il17f* promoter has not been previously characterized to our knowledge. We determined that the region 0.6 kb upstream of the *il17f* coding region contains a well defined TATA box and multiple ROR, AP-1, NFAT, and Runx1 consensus elements and was demethylated specifically in Th17 cells. Therefore, we used this region as the promoter in our study. Our results demonstrate that although the *il17a* promoter is responsive to STAT3 and Runx1, these factors exhibit no cooperativity at this promoter. Likewise, we show that the *il17f* promoter is moderately STAT3-responsive, highly ROR γ t-responsive, but by itself is also incapable of supporting synergy between STAT3, ROR γ t, and Runx1.

The -5-kb CNS and the +28-kb CNS exhibit permissive epigenetic marks and DNase hypersensitivity in activated Th17 cells (our studies and Ref. 14) and were able to enhance transcription from both promoters in transient reporter assays, indicating that these enhancers are part of the transcriptional architecture of the *il17a* and *il17f* multilocus region. The -5-kb CNS was previously shown to enhance transcription from a -2-kb *il17a* upstream construct in response to ROR γ t and Runx1 (5). Our studies confirm that the -5-kb enhancer is highly ROR γ t-responsive; however, this CNS was unable to enhance transcription from the minimal -0.6-kb promoter in response to either STAT3 or Runx1. The -5-kb CNS was also able to enhance transcription from the already highly ROR γ t-responsive *il17f* promoter, but did not respond to Runx1 or STAT3, individually or in combination. Therefore, we conclude that the primary role for the -5-kb enhancer is to coordinate ROR γ t activity and that another element must provide cooperativity to the *il17a-il17f* transcriptional unit.

It is possible that the action of multiple *cis* regulatory elements, although these elements are not capable of organizing cooperativity between STAT3, Runx1, and ROR γ t as a single element, might synergize to drive transcription when brought together in space. However, the combinatorial possibilities for

³ R. M. Thomas, H. Sai, and A. D. Wells, unpublished data.

Regulatory Architecture of the *il17* Locus

such cooperativity in *cis* within the ~120-kb *il17a-il17f* multi-locus region appears to be limited as our studies indicate that the -5-kb CNS and the promoters do not synergize under conditions of forced proximity and that the other intergenic CNS fail to exhibit enhancer activity in the context of either promoter. This could be explained by the fact that the -2.5-kb CNS retains a significant level of H3K27me3 mark in the Th17 lineage and contains no STAT3 or ROR consensus elements, and the +36-kb CNS exhibits low levels of H3K4me3 and DNase hypersensitivity in Th17 cells (our studies and Ref. 14), contains only a weak match for a STAT3 consensus element, and does not contain an ROR site. The +23 CNS is primed in Th17 cells (*i.e.* accumulates high levels of the H3K4me3 mark and loses H3K27me3), but contains no STAT3 nor ROR consensus elements. The -60 CNS contains a single, weak match for the STAT3 consensus and a single weak match for the ROR consensus, but this region remains epigenetically silent (*i.e.* high H3K27me3) in the Th17 lineage. The +10 CNS exhibits a strong change in H3K4 and H3K27 trimethylation and DNase hypersensitivity in Th17 cells (our studies and Ref. 14), contains a strong STAT consensus element, and binds STAT3 *in vivo* in activated Th17 cells (20). Why this element does not enhance in our system is not clear, but as with all these CNS, it is possible that additional factors not expressed in 293T cells may be required.

However, an excellent candidate for an element that *per se* supports cooperativity among the various factors required for IL-17 production is the +28-kb CNS, which we show is a strong enhancer of transcription from both the *il17a* and the *il17f* promoters. Although many of the CNS examined here exhibited DNase hypersensitivity in activated Th17 cells in the study by Mukasa *et al.* (14), the +28-kb CNS was the only CNS that showed constitutive hypersensitivity in resting Th17 cells, indicating the presence of a unique chromatin structure in this region. This enhancer shows strong STAT3 binding *in vivo* (20) and is highly responsive to STAT3 in our transient reporter assays. This enhancer is also responsive to ROR γ t and Runx1, but importantly, this enhancer is able to support transcriptional cooperativity between all three factors when expressed together. This CNS may also cooperate with additional DNA-binding proteins as this region also contains putative binding sites for SP1 and NFAT. Interestingly, one of these NFAT sites contains a CpG dinucleotide that we show is methylated in non-Th17 cells and unmethylated in Th17 cells. Methylation of an NFAT element has been shown to block NFAT binding and transactivation of the human *il2* promoter (27), suggesting that DNA methylation could act in an analogous manner at the *il17* loci to oppose NFAT-mediated transactivation. The +28-kb enhancer also contains multiple AP-1 consensus elements, suggesting that Fos/Jun heterodimers may act at this region. Alternatively, these sites may recruit Batf, an alternative Jun partner that was recently shown to be required for *il17a* gene expression (28). Indeed, this previous study demonstrated Batf binding to the endogenous +28 CNS region in Th17 cells, further indicating that this factor transactivates via interacting with the +28-kb enhancer. Therefore, we propose that the +28-kb enhancer is an integral component of the *il17a-il17f* transcriptional architecture that organizes the activity of multiple tran-

scription factors around the *il17a* and *il17f* promoters. Although this work does not strictly establish whether the +28-kb CNS is required for Th17 development, these studies do establish the element as a classically defined enhancer that can be targeted by homologous recombination in future studies.

In summary, we show that a conserved intergenic element can coordinate the activities of STAT3, ROR γ t, and Runx1 to enhance transcription from the *il17a* and *il17f* promoters and that Th17 cells utilize an evolutionarily conserved mechanism involving methylation at DNA binding elements to restrict STAT3 activity at the *il17a* gene in non-Th17 lineages.

Acknowledgments—We thank Drs. C. Hunter, Y. Chen, E. Rowell, and W. Hancock for helpful review of the manuscript.

REFERENCES

1. Torchinsky, M. B., Garaude, J., Martin, A. P., and Blander, J. M. (2009) Innate immune recognition of infected apoptotic cells directs Th17 cell differentiation. *Nature* **458**, 78–82
2. Iwakura, Y., Ishigame, H., Saijo, S., and Nakae, S. (2011) Functional specialization of interleukin-17 family members. *Immunity* **34**, 149–162
3. Hirahara, K., Ghoreschi, K., Laurence, A., Yang, X. P., Kanno, Y., and O’Shea, J. J. (2010) Signal transduction pathways and transcriptional regulation in Th17 cell differentiation. *Cytokine Growth Factor Rev.* **21**, 425–434
4. Rowell, E., Merckenschlager, M., and Wilson, C. B. (2008) Long-range regulation of cytokine gene expression. *Curr. Opin. Immunol.* **20**, 272–280
5. Zhang, F., Meng, G., and Strober, W. (2008) Interactions among the transcription factors Runx1, ROR γ t, and Foxp3 regulate the differentiation of interleukin 17-producing T cells. *Nat. Immunol.* **9**, 1297–1306
6. Takizawa, T., Nakashima, K., Namihira, M., Ochiai, W., Uemura, A., Yanagisawa, M., Fujita, N., Nakao, M., and Taga, T. (2001) DNA methylation is a critical cell-intrinsic determinant of astrocyte differentiation in the fetal brain. *Dev. Cell* **1**, 749–758
7. Bromberg, J. F., Wrzeszczynska, M. H., Devgan, G., Zhao, Y., Pestell, R. G., Albanese, C., and Darnell, J. E. (1999) Stat3 as an oncogene. *Cell* **98**, 295–303
8. Thomas, R. M., Gao, L., and Wells, A. D. (2005) Signals from CD28 induce stable epigenetic modification of the IL-2 promoter. *J. Immunol.* **174**, 4639–4646
9. Northrop, J. K., Thomas, R. M., Wells, A. D., and Shen, H. (2006) Epigenetic remodeling of the IL-2 and IFN γ loci in memory CD8 T cells is influenced by CD4 T cells. *J. Immunol.* **177**, 1062–1069
10. Thomas, R. M., Chunder, N., Chen, C., Umetsu, S. E., Winandy, S., and Wells, A. D. (2007) Ikaros enforces the costimulatory requirement for *IL2* gene expression and is required for anergy induction in CD4⁺ T lymphocytes. *J. Immunol.* **179**, 7305–7315
11. Langrish, C. L., Chen, Y., Blumenschein, W. M., Mattson, J., Basham, B., Sedgwick, J. D., McClanahan, T., Kastelein, R. A., and Cua, D. J. (2005) IL-23 drives a pathogenic T cell population that induces autoimmune inflammation. *J. Exp. Med.* **201**, 233–240
12. Yen, D., Cheung, J., Scheerens, H., Poulet, F., McClanahan, T., McKenzie, B., Kleinschek, M. A., Owyang, A., Mattson, J., Blumenschein, W., Murphy, E., Sathe, M., Cua, D. J., Kastelein, R. A., and Rennick, D. (2006) IL-23 is essential for T cell-mediated colitis and promotes inflammation via IL-17 and IL-6. *J. Clin. Invest.* **116**, 1310–1316
13. Bannister, A. J., and Kouzarides, T. (2011) Regulation of chromatin by histone modifications. *Cell Res.* **21**, 381–395
14. Mukasa, R., Balasubramani, A., Lee, Y. K., Whitley, S. K., Weaver, B. T., Shibata, Y., Crawford, G. E., Hatton, R. D., and Weaver, C. T. (2010) Epigenetic instability of cytokine and transcription factor gene loci underlies plasticity of the T helper 17 cell lineage. *Immunity* **32**, 616–627
15. Akimzhanov, A. M., Yang, X. O., and Dong, C. (2007) Chromatin remod-

- eling of interleukin-17 (IL-17)-IL-17F cytokine gene locus during inflammatory helper T cell differentiation. *J. Biol. Chem.* **282**, 5969–5972
16. Wei, G., Wei, L., Zhu, J., Zang, C., Hu-Li, J., Yao, Z., Cui, K., Kanno, Y., Roh, T. Y., Watford, W. T., Schones, D. E., Peng, W., Sun, H. W., Paul, W. E., O'Shea, J. J., and Zhao, K. (2009) Global mapping of H3K4me3 and H3K27me3 reveals specificity and plasticity in lineage fate determination of differentiating CD4⁺ T cells. *Immunity* **30**, 155–167
 17. Ichiyama, K., Yoshida, H., Wakabayashi, Y., Chinen, T., Saeki, K., Nakaya, M., Takaesu, G., Hori, S., Yoshimura, A., and Kobayashi, T. (2008) Foxp3 inhibits ROR γ t-mediated IL-17A mRNA transcription through direct interaction with ROR γ t. *J. Biol. Chem.* **283**, 17003–17008
 18. Yang, X. O., Panopoulos, A. D., Nurieva, R., Chang, S. H., Wang, D., Watowich, S. S., and Dong, C. (2007) STAT3 regulates cytokine-mediated generation of inflammatory helper T cells. *J. Biol. Chem.* **282**, 9358–9363
 19. Zhou, L., Ivanov, I. I., Spolski, R., Min, R., Shenderov, K., Egawa, T., Levy, D. E., Leonard, W. J., and Littman, D. R. (2007) IL-6 programs Th17 cell differentiation by promoting sequential engagement of the IL-21 and IL-23 pathways. *Nat. Immunol.* **8**, 967–974
 20. Yang, X. P., Ghoreschi, K., Steward-Tharp, S. M., Rodriguez-Canales, J., Zhu, J., Grainger, J. R., Hirahara, K., Sun, H. W., Wei, L., Vahedi, G., Kanno, Y., O'Shea, J. J., and Laurence, A. (2011) Opposing regulation of the locus encoding IL-17 through direct, reciprocal actions of STAT3 and STAT5. *Nat. Immunol.* **12**, 247–254
 21. Yang, X. O., Pappu, B. P., Nurieva, R., Akimzhanov, A., Kang, H. S., Chung, Y., Ma, L., Shah, B., Panopoulos, A. D., Schluns, K. S., Watowich, S. S., Tian, Q., Jetten, A. M., and Dong, C. (2008) T helper 17 lineage differentiation is programmed by orphan nuclear receptors ROR α and ROR γ . *Immunity* **28**, 29–39
 22. Walsh, C. P., and Bestor, T. H. (1999) Cytosine methylation and mammalian development. *Genes Dev.* **13**, 26–34
 23. Schindler, C., and Darnell, J. E. (1995) Transcriptional responses to polypeptide ligands: the JAK-STAT pathway. *Annu. Rev. Biochem.* **64**, 621–651
 24. Chen, Z., Laurence, A., Kanno, Y., Pacher-Zavisin, M., Zhu, B. M., Tato, C., Yoshimura, A., Hennighausen, L., and O'Shea, J. J. (2006) Selective regulatory function of Socs3 in the formation of IL-17-secreting T cells. *Proc. Natl. Acad. Sci. U.S.A.* **103**, 8137–8142
 25. Jacobson, N. G., Szabo, S. J., Weber-Nordt, R. M., Zhong, Z., Schreiber, R. D., Darnell, J. E., Jr., and Murphy, K. M. (1995) Interleukin 12 signaling in T helper type 1 (Th1) cells involves tyrosine phosphorylation of signal transducer and activator of transcription (Stat)3 and Stat4. *J. Exp. Med.* **181**, 1755–1762
 26. Hirota, K., Duarte, J. H., Veldhoen, M., Hornsby, E., Li, Y., Cua, D. J., Ahlfors, H., Wilhelm, C., Tolaini, M., Menzel, U., Garefalaki, A., Potocnik, A. J., and Stockinger, B. (2011) Fate mapping of IL-17-producing T cells in inflammatory responses. *Nat. Immunol.* **12**, 255–263
 27. Murayama, A., Sakura, K., Nakama, M., Yasuzawa-Tanaka, K., Fujita, E., Tateishi, Y., Wang, Y., Ushijima, T., Baba, T., Shibuya, K., Shibuya, A., Kawabe, Y., and Yanagisawa, J. (2006) A specific CpG site demethylation in the human interleukin 2 gene promoter is an epigenetic memory. *EMBO J.* **25**, 1081–1092
 28. Schraml, B. U., Hildner, K., Ise, W., Lee, W. L., Smith, W. A., Solomon, B., Sahota, G., Sim, J., Mukasa, R., Cemurski, S., Hatton, R. D., Stormo, G. D., Weaver, C. T., Russell, J. H., Murphy, T. L., and Murphy, K. M. (2009) The AP-1 transcription factor Batf controls Th17 differentiation. *Nature* **460**, 405–409